NUMERICAL SIMULATION OF AIR FLOW THROUGH TWO DIFFERENT SHAPED AIR VENTS

Catalin-Adrian Neacsu[1], Mariana Ivanescu, Ion Tabacu

INTRODUCTION

Most car manufacturers gives a lot of attention in the shape of interior components such as dashboard, steering wheel, different setting knobs, seats and even air inlets. The later represent a challenge because they must allow the car occupants to easy direct the air flow and also to provide a good distribution of air inside the cabin [1], [4].

In the recent years, one tool that is often used in the field of airflow numerical simulation is represented by the computational fluid dynamics (CFD). It has proved its efficiency in various applications including also the automotive field. We can find CFD used in applications concerning the airflow around cars, inside car airflow, and also the simulation of the engine functioning.

In our paper, we will use CFD to simulate the air flow through two different shaped air flow vents with the same external area and to analyze the air distribution at various distances, starting from 100 to 500mm from the outlet of the air vent. For the numerical simulation we will use the Fluent 6.3.26 software, because it's proved capability to solve problems concerning the air flow. The 3D model of the air vents was created in Catia V5, using measurements taken from the physical parts, and the finite element model used was created using the Beta Cae ANSA software.

BRIEF INTRODUCTION TO FLUENT

Fluent code contains all the physical capabilities needed to model flow, turbulence, heat transfer and reactions for industrial applications[2],[6]. It uses a finite volume approach to solve the equations governing the flow and is widely used in numerical simulations of different flow conditions of various complexities. It is chosen in this study because its proven capability and validity in flows similar to those investigated here. The turbulent flow fields are calculated by solving the Reynolds averaged three-dimensional Navier-Stokes equations along with the continuity equation (1) and (2)[3],[5],[7],[8],[9].

[1] Corresponding author e-mail: catalin.neacsu@renault.com; Automobile Dacia - Group Renault Romania

(1):

$$\frac{\partial \bar{u}}{\partial t} + \bar{u}\frac{\partial (\bar{u})}{\partial x} + \bar{v}\frac{\partial (\bar{u})}{\partial y} + \bar{w}\frac{\partial (\bar{u})}{\partial z} = X - \frac{1}{\rho}\frac{\partial \bar{p}}{\partial x} + \nu\Delta\bar{u} + \frac{1}{\rho}\left(\frac{\partial}{\partial x}\left(-\rho\overline{u'u'}\right) + \frac{\partial}{\partial y}\left(-\rho\overline{v'u'}\right) + \frac{\partial}{\partial z}\left(-\rho\overline{w'u'}\right)\right)$$

$$\frac{\partial \bar{v}}{\partial t} + \bar{u}\frac{\partial (\bar{v})}{\partial x} + \bar{v}\frac{\partial (\bar{v})}{\partial y} + \bar{w}\frac{\partial (\bar{v})}{\partial z} = Y - \frac{1}{\rho}\frac{\partial \bar{p}}{\partial y} + \nu\Delta\bar{v} + \frac{1}{\rho}\left(\frac{\partial}{\partial x}\left(-\rho\overline{u'v'}\right) + \frac{\partial}{\partial y}\left(-\rho\overline{v'v'}\right) + \frac{\partial}{\partial z}\left(-\rho\overline{w'v'}\right)\right)$$

$$\frac{\partial \bar{w}}{\partial t} + \bar{u}\frac{\partial (\bar{w})}{\partial x} + \bar{v}\frac{\partial (\bar{w})}{\partial y} + \bar{w}\frac{\partial (\bar{w})}{\partial z} = Z - \frac{1}{\rho}\frac{\partial \bar{p}}{\partial z} + \nu\Delta\bar{w} + \frac{1}{\rho}\left(\frac{\partial}{\partial x}\left(-\rho\overline{u'w'}\right) + \frac{\partial}{\partial y}\left(-\rho\overline{v'w'}\right) + \frac{\partial}{\partial z}\left(-\rho\overline{w'w'}\right)\right)$$

$$\frac{\partial \bar{u}}{\partial x} + \frac{\partial \bar{v}}{\partial y} + \frac{\partial \bar{w}}{\partial z} = 0 \qquad\qquad (2)$$

To solve the equations (1) and (2) have been developed various approaches, one of the most used being the use of two equations model. The k-ε model is one of the most used turbulence model, and it includes two extra transport equations to represent the turbulent properties of the flow. This allows a two equation model to account for history effects like convection and diffusion of turbulent energy.

The first transported variable is turbulent kinetic energy, k and the second transported variable in this case is the turbulent dissipation, ε. It is the variable that determines the scale of the turbulence, whereas the first variable, k, determines the energy in the turbulence[6].

In the Fluent software the user can choose from three types of k- ε model solver: Standard, RNG and Realizable, each one with its own mathematical expression, and in our simulation we will use the Realizable k- ε model, because it satisfies specific constraints that make the model more consistent with the physics of turbulent flows, and give more accurate results than the Standard k- ε model[6].

GEOMETRY PREPARATION

Starting from the measurements taken from the real pieces we have realized the 3D model of the air inlets using CATIA software, and we have scaled them to have the same frontal area, which will be of $0.006m^2$, the surface being the same for the air flow entrance in the inlet.

After the CAD creation, we have used the Beta CAE Ansa to obtain the surface mesh of the air inlets, mesh that can be seen in figure 1 and 2.
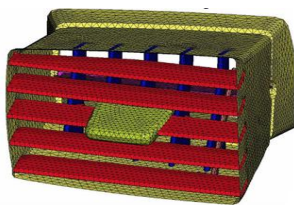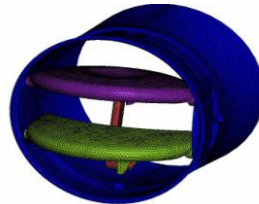

Figure 1: *Rectangular shaped air inlet*   **Figure 2:** *Round shaped air inlet*

In table 1 we can see a short description of the finite element model for both types of vents.

Table 1: *Description of the finite element model*

Shape	*Rectangular*	*Round*
Type of elements	*Only tria*	*Only tria*
Number of elements	~ 60000	~ 40000
Medium size of mesh	1mm	1.2mm

Comparing those two air vents, we can observe that the rectangular shaped vent is more complex, having a lot more components than the rounded shaped vent, thus giving us a bigger number of triangular elements on the domain, with about 50% more than the round shaped model.

Because we will want to analyse the flow at different distances from the air vent, we must construct an additional geometry, in which the air will flow, and this will be our post-processing domain. The shape of the geometry is given in figure 3(with the rectangular vent integrated), and it will be an extruded isoscel trapeze with the base of 800mm, the short edge of 200mm and a height of 1000mm. The extrusion will be of 800mm, the centre of inlet being positioned at the centre of the upper face, as we can see in figure 3. The same shape is used also in [1].
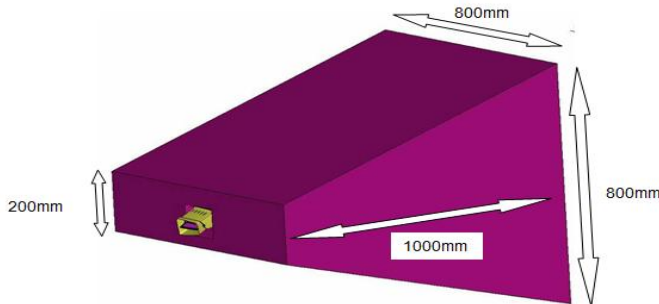

Figure 3: *Computational domain*

With the computational domain defined and the vent included, we will create the volume discretization of domain obtaining around 0.75×10^6 elements for the rounded shape vent and around 1.2×10^6 elements for the rectangular shaped vent.

BOUNDARY CONDITIONS AND FLUENT SET-UP

Because we will simulate numerically the air flow through the vents we will need to define the boundary conditions at the inlets, thus being given by a flow rate. To determine the type of flow, we must also compute the Reynolds number for each type of flow, with the formula (3) [5].

$$\mathrm{Re} = \frac{QD_H}{vA}$$ (3)

where: Q – Volumetric flow rate (m^3/s)

D_H – Hydraulic diameter (m)

v – Kinematic viscosity (m^2/s) - 15.68x10^{-6} m^2/s for air

A – Cross sectional area of the entry domain (m^2)

The values for the flow rate and Reynolds number for each flow can be seen in table 2.

Table 2: *Flow rate with corresponding Reynolds number*

Air flow rate(m^3/s)	0.075		0.040	
Type of inlet	Rectangular	Round	Rectangular	Round
Area (m^2)	0.0057	0.0060	0.0057	0.0060
Hydraulic diameter(m)	0.307	0.273	0.307	0.273
Reynolds(Re) number	257619	217633	137397	116071
Type of flow (based on Re)	Turbulent	Turbulent	Turbulent	Turbulent

Based on the Reynolds number, we can establish that the flow is turbulent; we can now set up the Fluent solver. We will use, as we mentioned, the Realizable k- ε model for solving the turbulent flow, and we will define the inlet boundary condition as a mass-flow inlet and the outlet as a pressure outlet. For the mass flow inlet we will use the values in the table 2, as for the outlet we will consider the atmospheric pressure.

RESULTS

With the specified boundary conditions, we will have four simulations, two for each type of vent. We will analyse the air flow magnitude on central axis of the boundary domain (intersection of the planes Y=0 and Z=0) and also the distribution on sectional planes as we can see in figure 4.
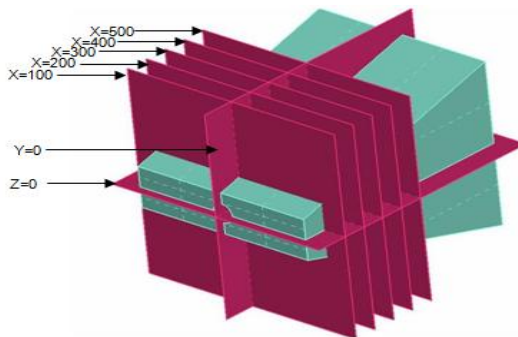

Figure 4: *Post-processing planes*

In table 3 we can see the velocity values obtained for the speed in all four simulations and in figure 5 we can see the graphs of velocity.

Table 3: *Velocities along the domain centreline*

Air flow rate(m³/s)	0.075			0.040		
Type of inlet	*Rectangular*	*Round*	*Difference*	*Rectangular*	*Round*	*Difference*
	Speed(m/s)		*(m/s)*	*Speed(m/s)*		*(m/s)*
x= 50mm	6.81	6.30	+0.51	12.79	11.72	+1.07
x=100mm	6.51	5.73	+0.78	12.41	10.75	+1.66
x=150mm	5.25	4.41	+0.84	9.85	8.24	+1.61
x=200mm	4.49	3.43	+1.06	8.43	6.40	+2.03
x=250mm	3.86	3.02	+0.84	7.24	5.60	+1.64
x=300mm	3.36	2.72	+0.64	6.31	5.06	+1.25
x=350mm	3.09	2.31	+0.78	5.82	4.31	+1.51
x=400mm	2.88	2.19	+0.69	5.43	4.07	+1.36
x=450mm	2.73	1.95	+0.78	5.13	3.60	+1.53
x=500mm	2.57	1.78	+0.79	4.84	3.28	+1.56
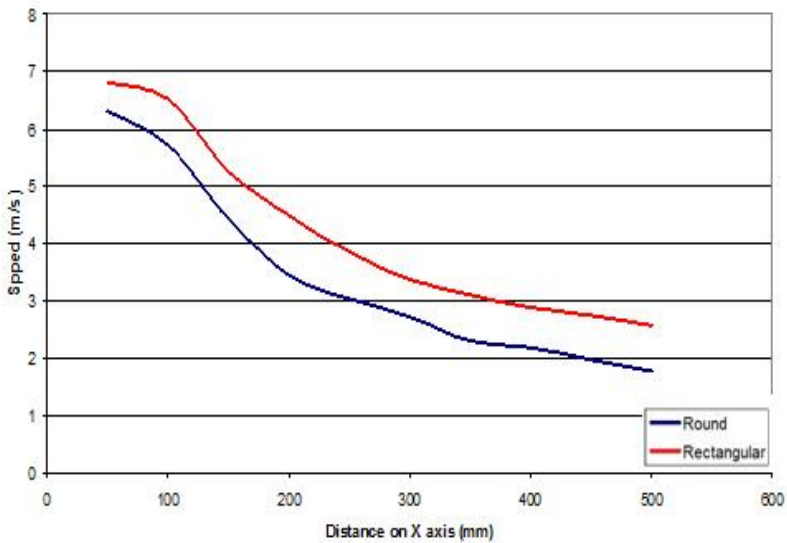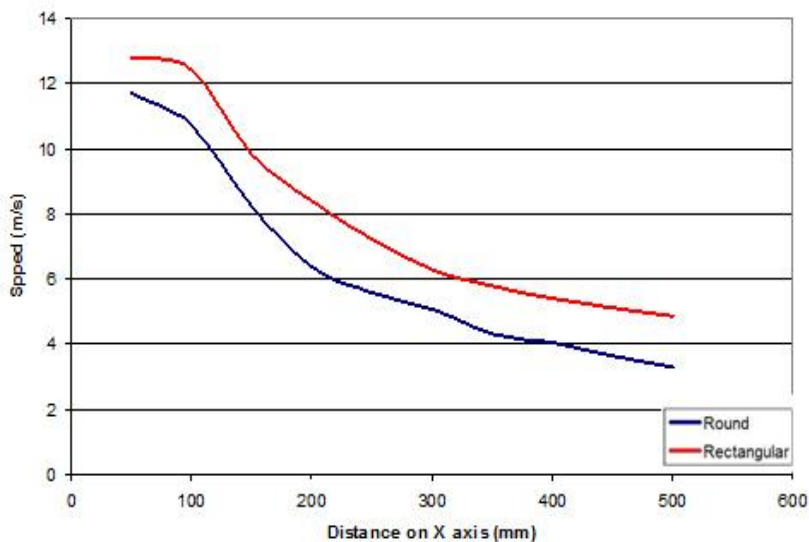
Figure 5: *Graphics of velocity on the centreline (0.04m³/s left; 0.075m³/s right)*

Analyzing the obtained results, we observe a difference between the results obtained with the rectangular shaped vent and round shaped vent. This difference can be explained by the different obstructed area from the internal components of the air vents. The internal components of the round shaped air inlet obstruct an area of $0.0016m^2$ whilst the internal components of the rectangular shaped $0.0021m^2$, this can be seen in figure 6. The area obstructed refers to the projected area of the last fins on the perpendicular plane.
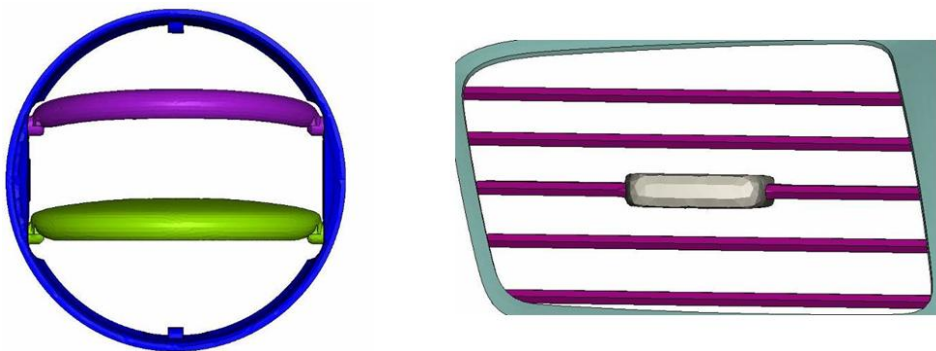

Figure 6: *Obstructed area for both type of vents*

In figures 7 and 8 we can see the cartographies of air distribution in the sectional planes y=0mm and z=0mm for the two flow rates given, and in figure 9 and 10 we can see the air distribution in planes x from 100 to 500 mm.

Plane
y=0

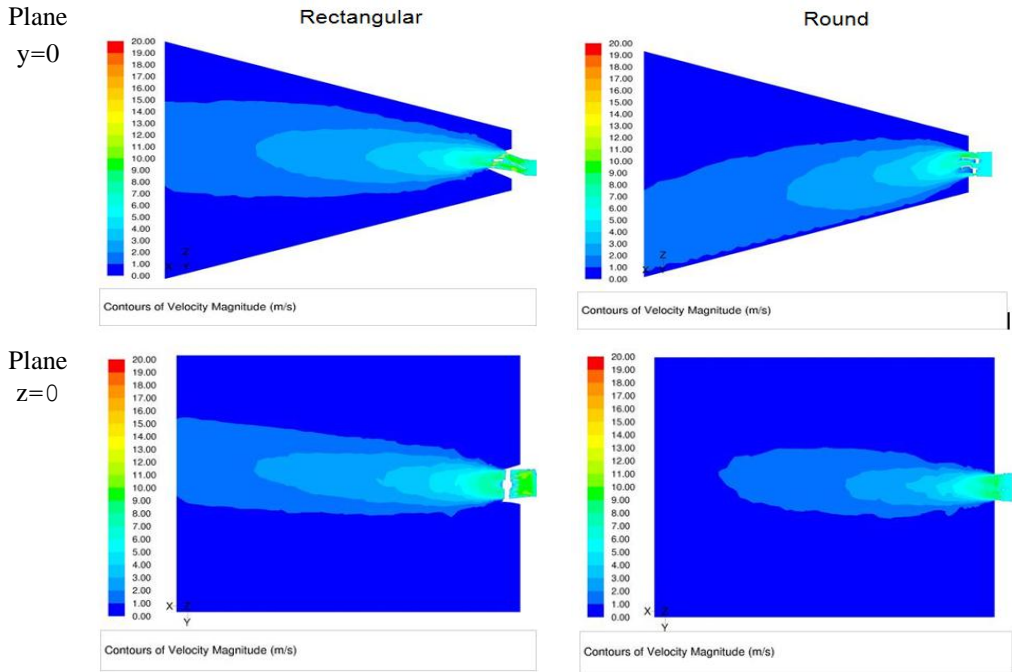Rectangular   Round

Plane
z=0

Figure 7: *Cartographies of velocities in planes y and z for an air flow rate of 0.040m3/s*

Plane
y=0

Rectangular   Round

Plane
z=0

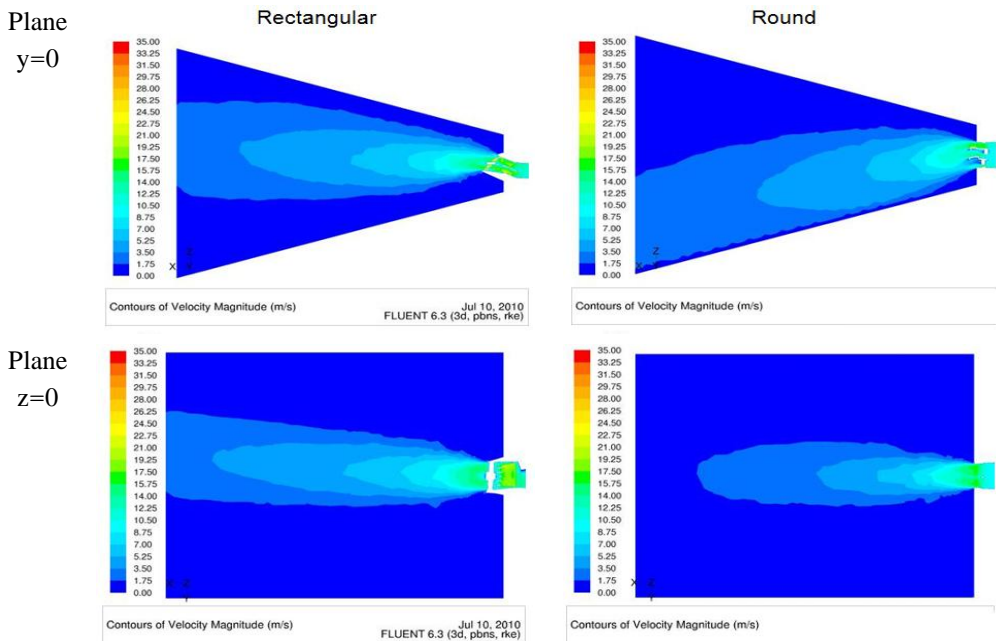**Figure 8:** *Cartographies of velocities in planes y and z for an air flow rate of 0.075m^3/s*
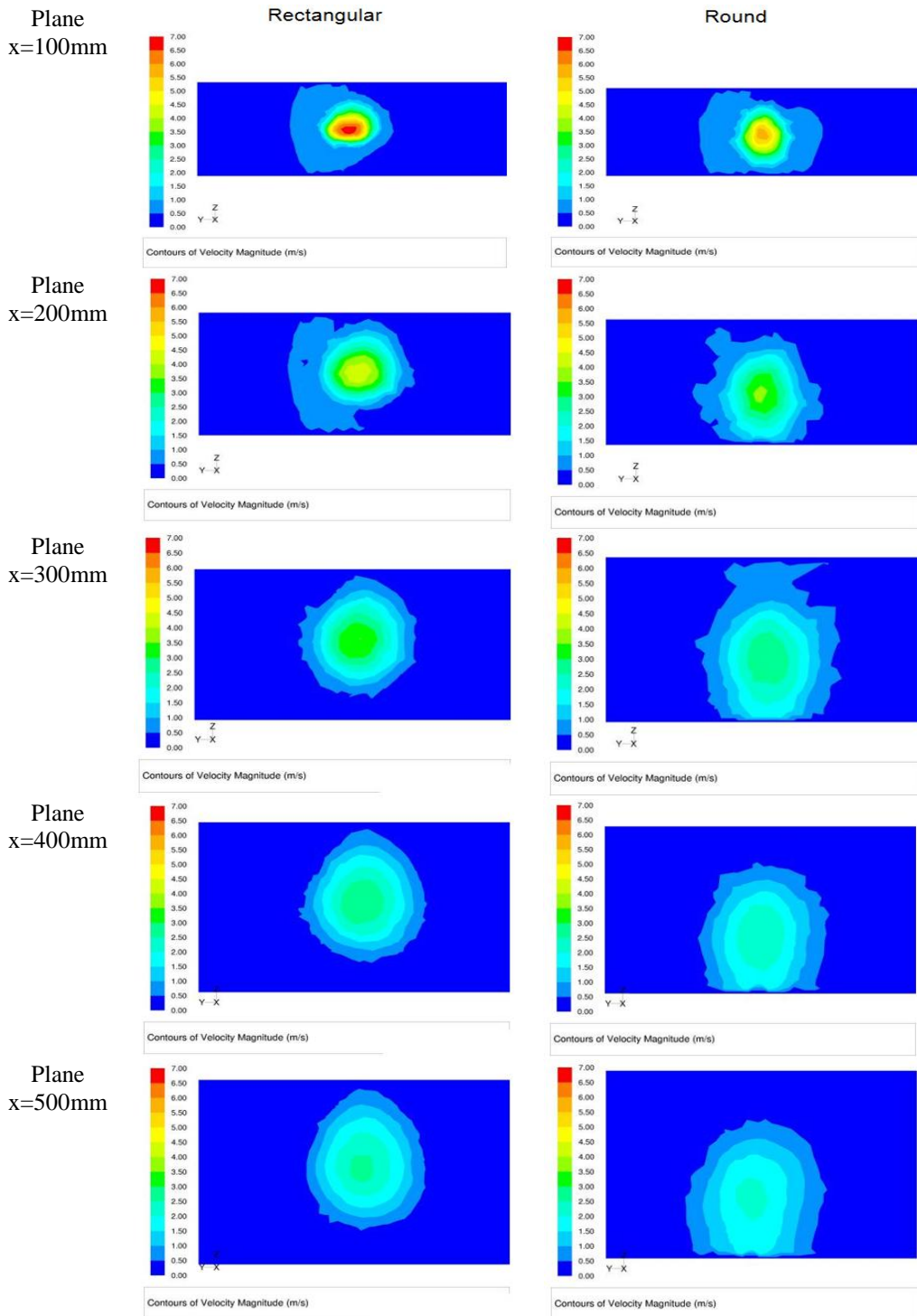
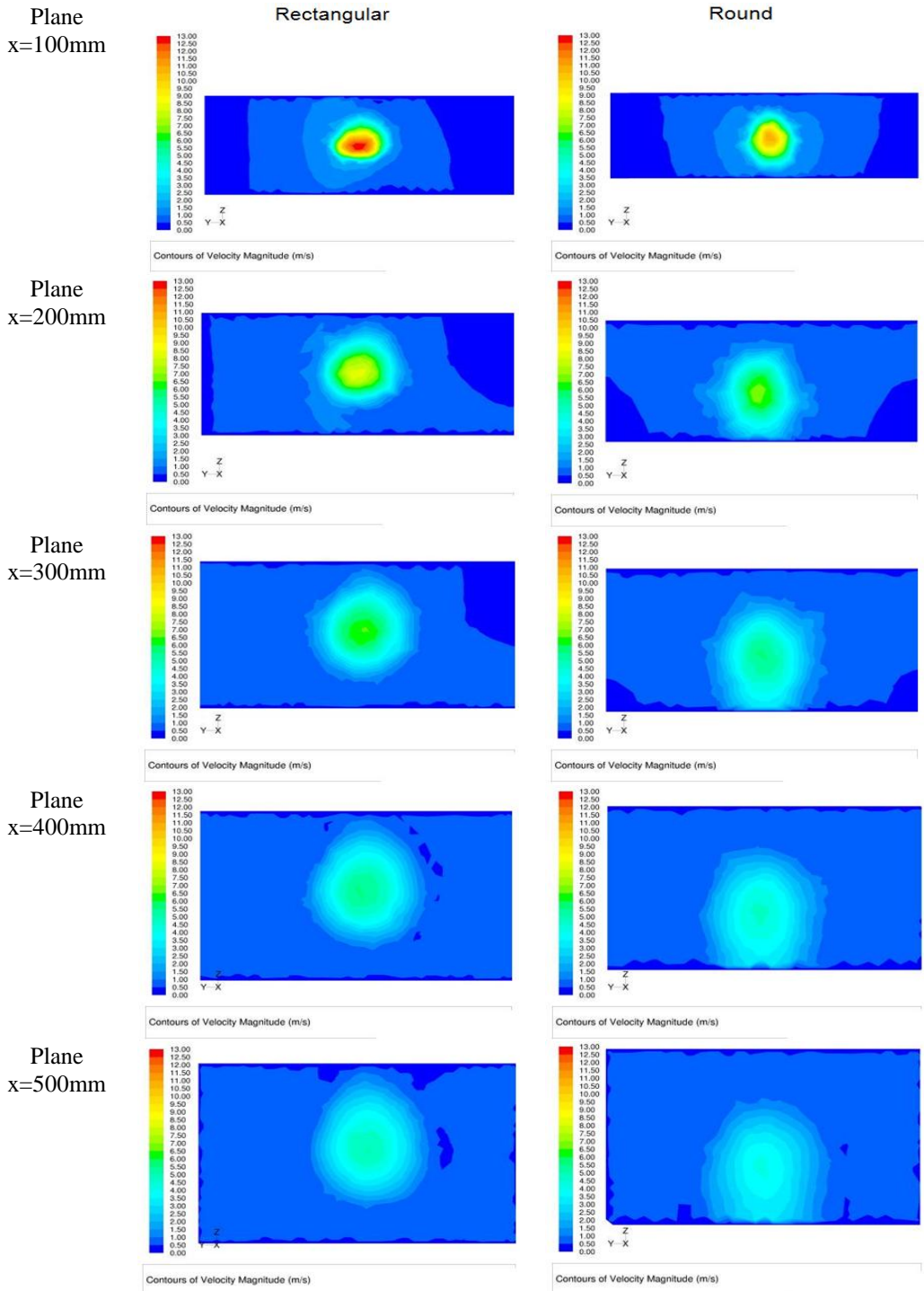**Figure 9:** *Cartographies of velocities in planes x from 100 to 500mm for an air flow rate of $0.040m^3/s$*

Figure 10: *Cartographies of velocities in planes x from 100 to 500mm*
for an air flow rate of $0.075m^3/s$

Also, from figures 7 to 10 we can see that in the case of the rounded shaped vent, the air is directed mainly downward, although the upper side of the fins is parallel with the plane Z=0. The path can be explained by the existence of a rounded surface at the outer extremities, as we can see in figure 11. Here we can see the vectors in the plane Y=0, and we can observe that the vectors are directed slightly downward.
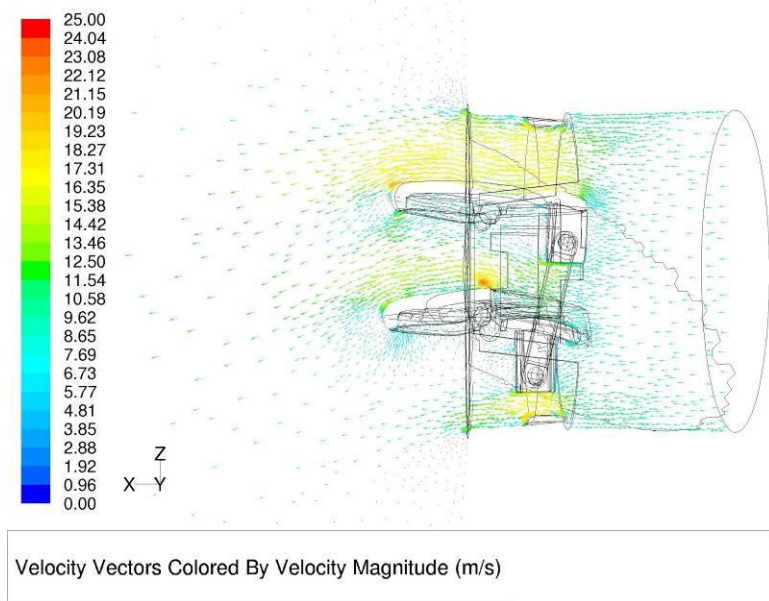

Figure 11: Velocity vectors at the exit of the inlet in the plane with XOY

CONCLUSIONS

Analyzing the obtained results, we can see that beside the aesthetic role, the air vents also have an role in the air distribution inside car cockpit, different shape giving us different results.

The first conclusion is that for the same frontal area, the exit speed of air is greater in the case of the rectangular inlet than the round, for the same quantity of air entered. To obtain the same velocity of air for the rectangular and round air inlets we have multiple opportunities:

- increasing the area of the rectangular inlet, thus giving us also a bigger area covered by the air inside the cockpit;
- decreasing the quantity of air needed in the case of the rectangular vent, this giving us a gain in the energy needed for the ventilation system.

Also, analyzing the results obtained in the case of the round air inlet vent, we can observe that small details of the fins can change the trajectory of the exiting air.

REFERENCES

[1] Axelsson Niklas and Enwald Hans, "Accuracy in flow simulation of climate control – Part I: The air distribution system", SAE 1999-01-1200

[2] Broboana D., Muntean T., Balan C.: " Mecanica fluidelor cu FLUENT-vol 1", Ed. Politehnica, Bucuresti, 2005

[3] Cebeci T., Shao J.P., Kafyeke F., Laurendeau E., "Computational Fluid Dynamics for Engineers", Horizons Publishing Inc. USA, 2005

[4] Currle J., Maue J. "Numerical study of the influence of air vent area and air mass flux on the thermal comfort of car occupants", SAE 2000-01-0980

[5] Florea J., Panaitescu V. : " Mecanica Fluidelor" – Editura Didactica si Pedagogica Bucuresti, 1979

[6] Fluent 6.3.26 Users Guide

[7] Hirsch C. "Numerical computation of internal and external flows", Volume 1, Fundamentals of Computational Fluid Dynamics, Butterworth-Heinemann, 2007

[8] Petrila T.,Trif D.: " Basics of fluid mechanics and introduction to computational fluid dynamics   ", Springer, 2004

[9] White F.M. "Fluid Mechanics", 4th ed. The McGraw Companies, 2001